Supporting Information

Photo-assisted hydrothermal synthesis of IrOx-TiO_2 for enhanced water oxidation

Ping Li,[a] Lingqiao Kong,[a] Jing Liu,[a] Junqing Yan,[a]* and Shengzhong Liu[a,b]*

a) Key Laboratory of Applied Surface and Colloid Chemistry, Ministry of Education, Shaanxi Key Laboratory for Advanced Energy Devices, Shaanxi Engineering Lab for Advanced Energy Technology, School of Materials Science and Engineering, Shaanxi Normal University, Xi'an, 710119, People's Republic of China.
E-mail: junqingyan@snnu.edu.cn

b) iChEM, Dalian Institute of Chemical Physics, Dalian National Laboratory for Clean Energy, Chinese Academy of Sciences, Dalian, 116023, People's Republic of China.
E-mail: liusz@snnu.edu.cn

Number of pages: 18

Number of figures:15

Number of tables: 3

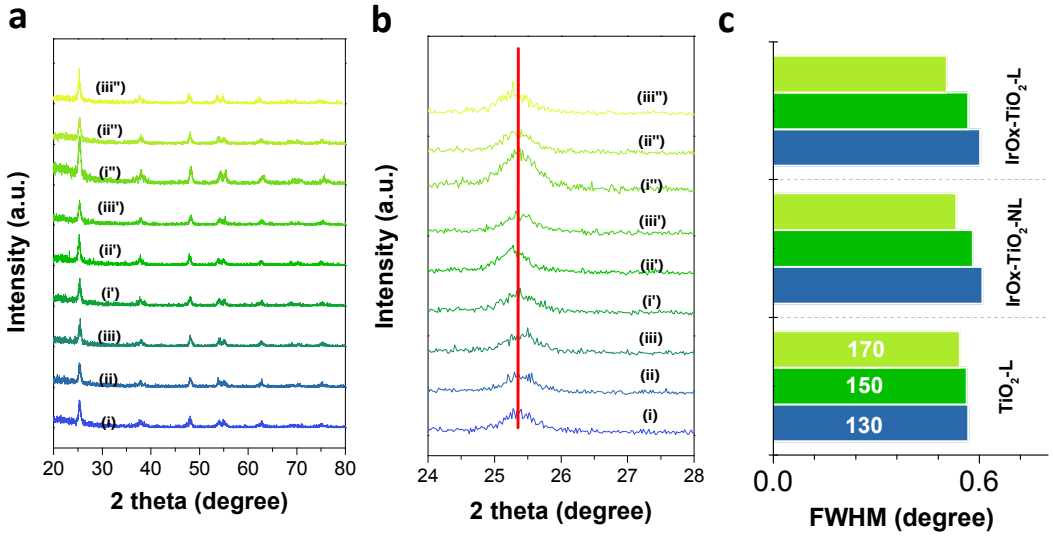

Figure S1. XRD results of the IrOx-TiO_2 samples obtained from different preparation conditions. (a) XRD patterns, i-iii: TiO_2-130-L, TiO_2-150-L, TiO_2-170-L; i'-iii': IrOx-TiO_2-130-NL, IrOx-TiO_2-150-NL, IrOx-TiO_2-170-NL; i''-iii'': IrOx-TiO_2-130-L, IrOx-TiO_2-150-L, IrOx-TiO_2-170-L. (b) The enlarge region at 2 theta of 24 to 28 degree and (c) the corresponding full width at half maximum (FWHM) values of the peak (101) at 2 theta of 25.3 degree.

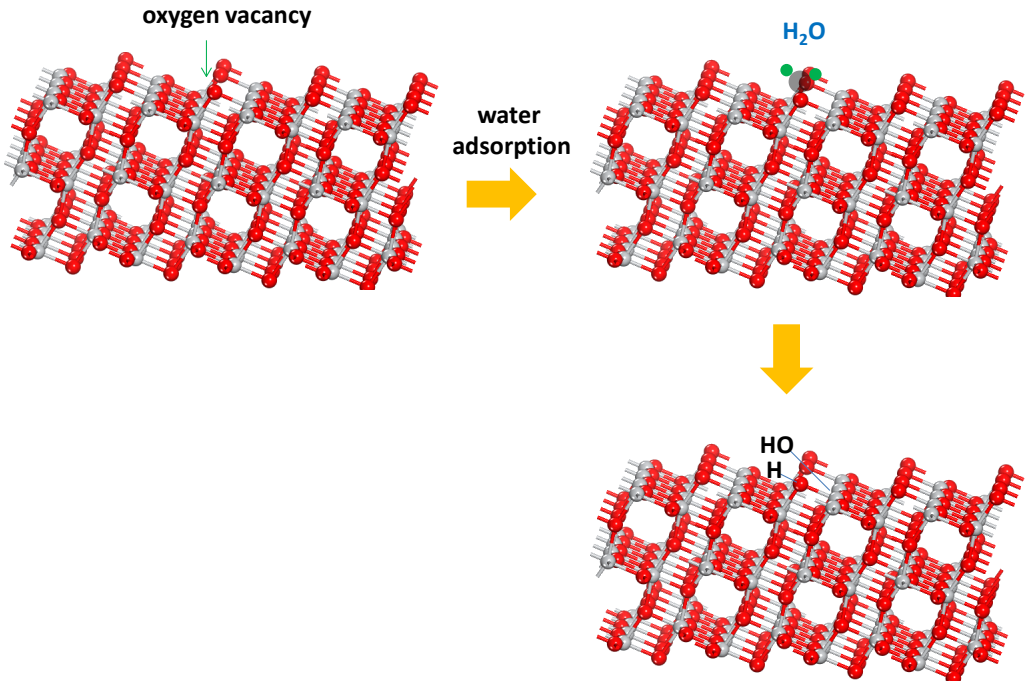

Figure S2. The formation process of two types of surface OH.

Table S1. The relative percentage of the three oxygen-based peaks (%).

Sample	Lattice O	OH group	Adsorbed water
IrOx-TiO_2-130-L	74.869	14.765	10.366
IrOx-TiO_2-150-L	51.891	46.233	1.877
IrOx-TiO_2-170-L	95.644	2.568	1.788

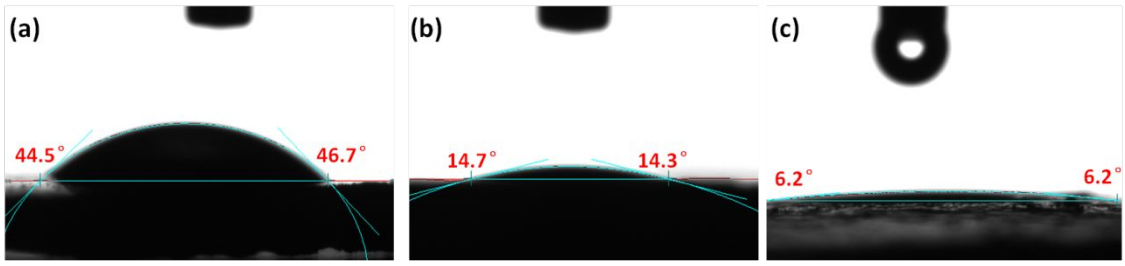

Figure S3. The contact angles of (a) TiO_2-150-NL, (b) TiO_2-150-L and (c) IrOx-TiO_2-150-L.

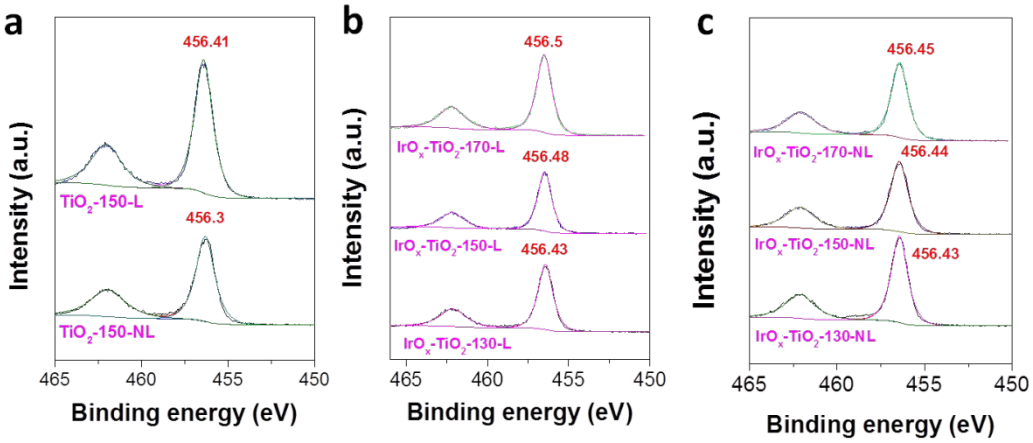

Figure S4. Ti 2p XPS results of the studied samples.

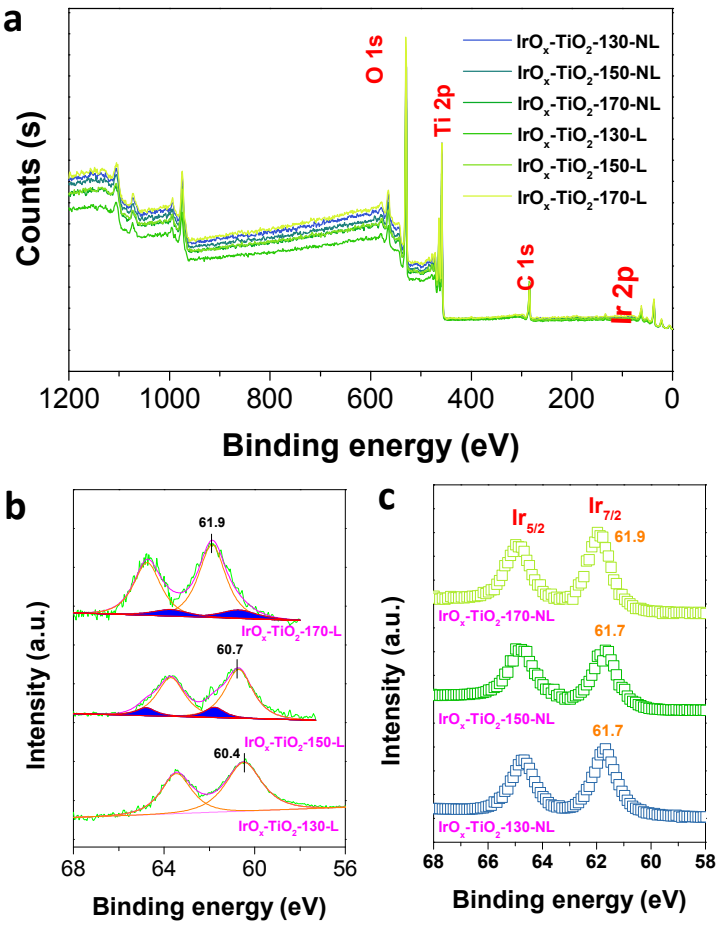

Figure S5. (a) The wide XPS results, (b)-(c) the Ir 4f results of IrOx-TiO_2 based samples under illumination and dark conditions.

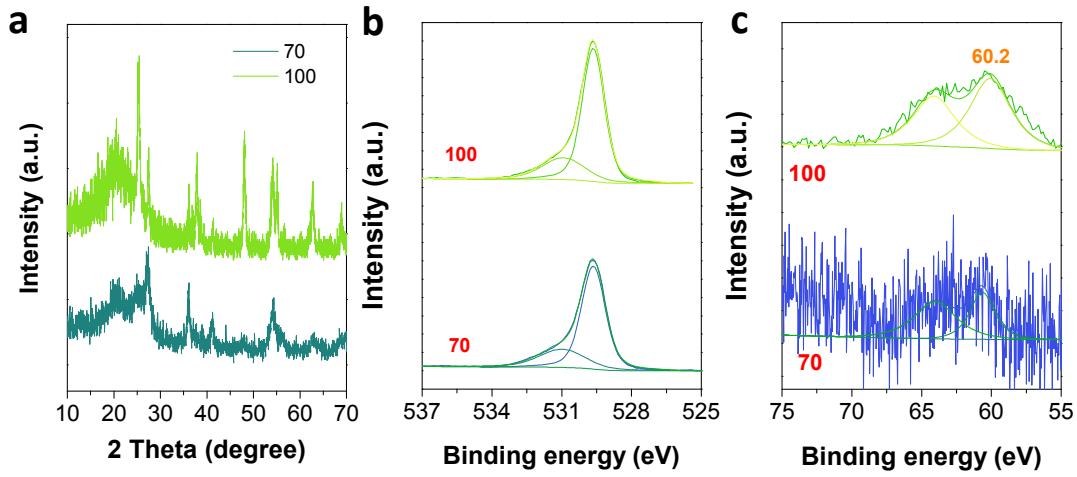

Figure S6. The physical properties of the two samples obtained from 70 and 100 ˚C. (a) XRD patterns, (b) O 1s XPS and (c) Ir 4f XPS results.

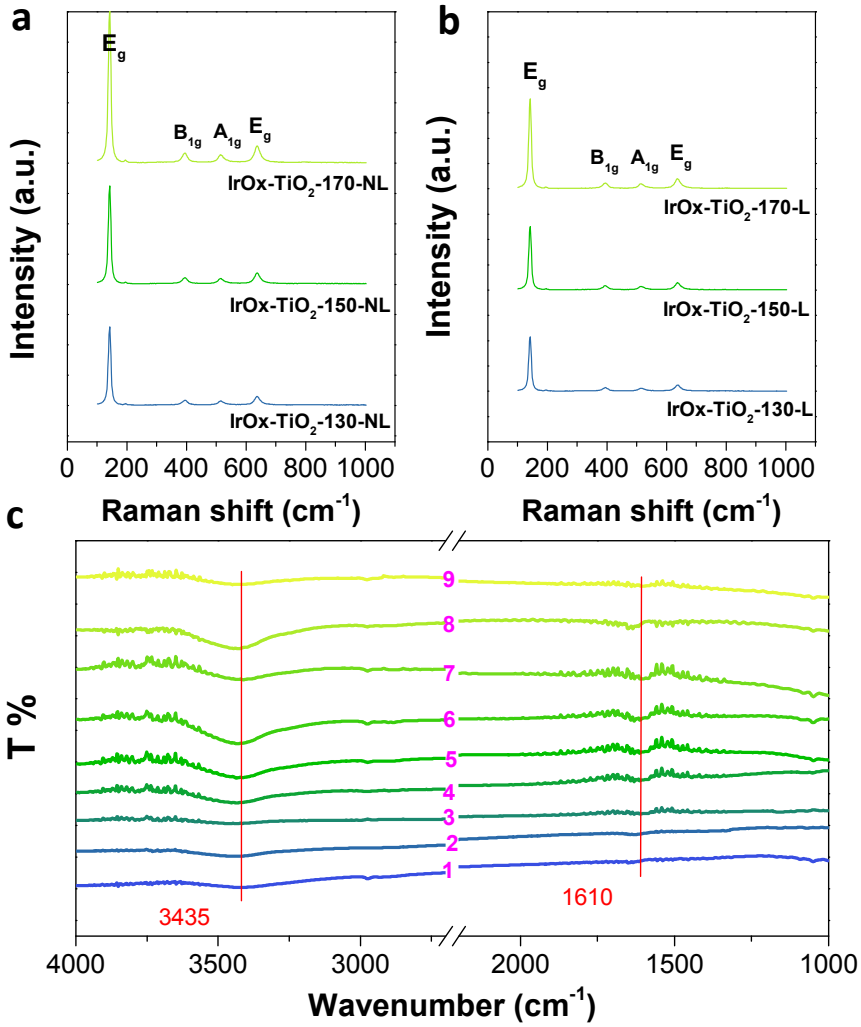

Figure S7. Raman spectra of (a) IrOx-TiO_2-NL samples and (b) IrOx-TiO_2-L samples. (c) FTIR spectrum of the studied samples: 1, TiO_2-170-L; 2, TiO_2-150-L; 3, TiO_2-150-NL; 4-6, IrOx-TiO_2-130-L, IrOx-TiO_2-150-L, IrOx-TiO_2-170-L; 7-9, IrOx-TiO_2-130-NL, IrOx-TiO_2-150-NL, IrOx-TiO_2-170-NL.

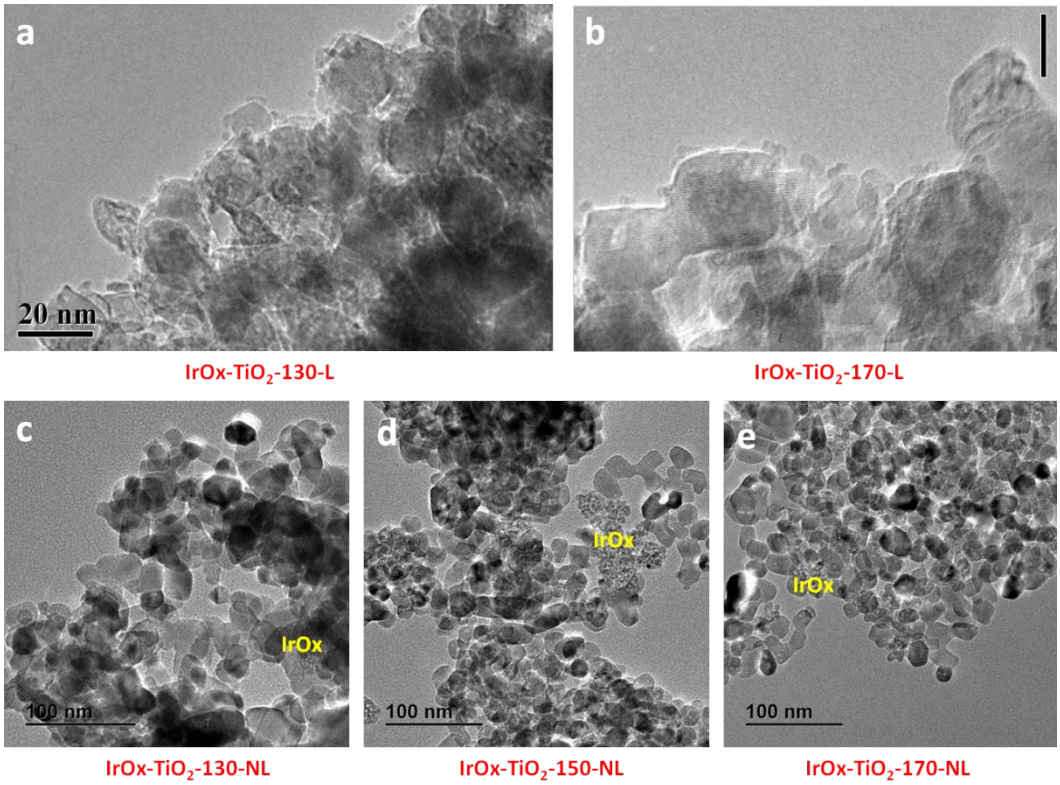

Figure S8. (a)-(b) TEM image of IrOx-TiO_2-130-NL and IrOx-TiO_2-170-L samples, (c)-(e) TEM images of IrOx-TiO_2-130-NL, IrOx-TiO_2-150-NL and IrOx-TiO_2-170-NL.

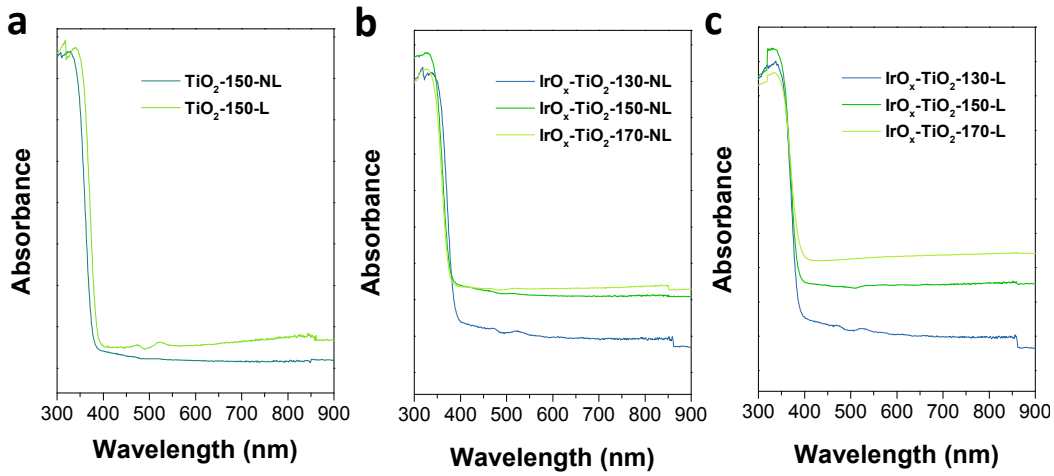

Figure S9.UV-vis absorption spectroscopy, (a) TiO_2-150-NL, TiO_2-150-NL; (b) IrOx-TiO_2-130-NL, IrOx-TiO_2-150-NL and IrOx-TiO_2-170-NL; (c) IrOx-TiO_2-130-L, IrOx-TiO_2-150-L and IrOx-TiO_2-170-L.

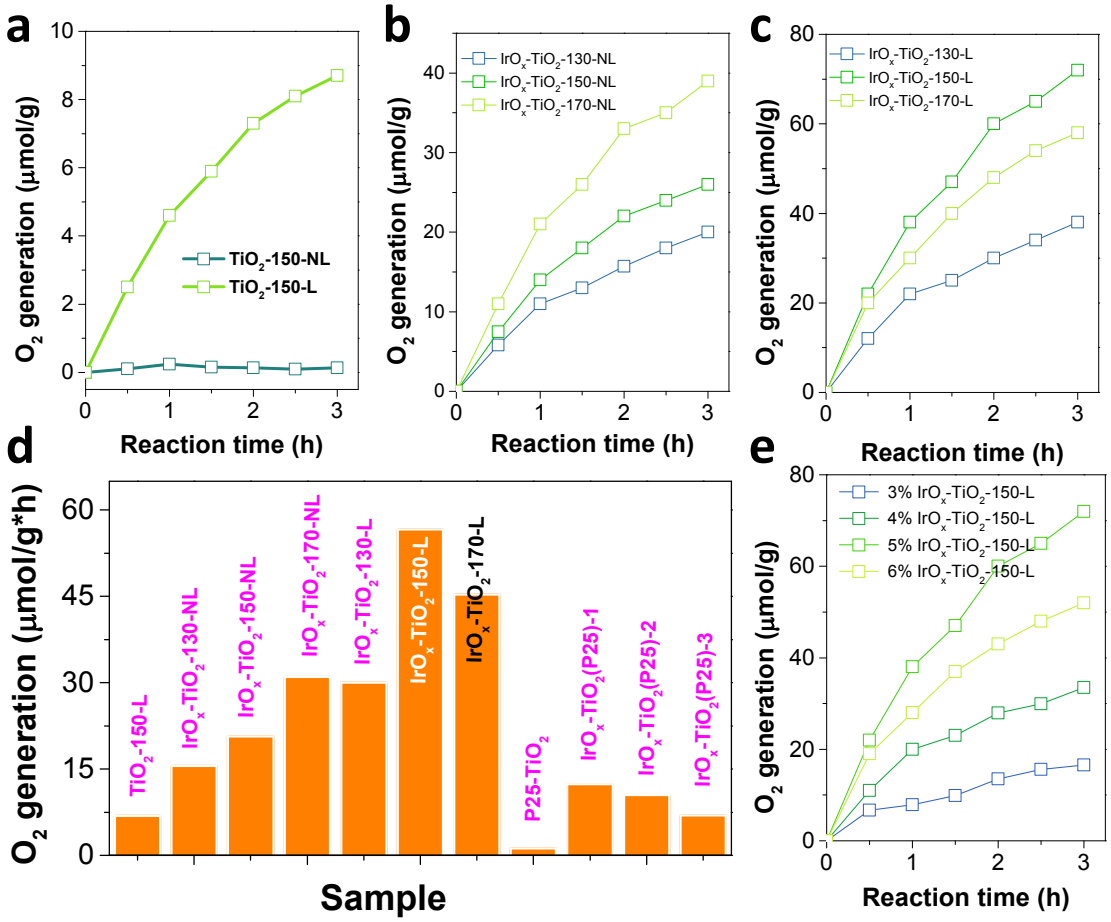

Figure S10. Photocatalytic water oxidation performance. (a) TiO_2-150-NL and TiO_2-150-L; (b) IrOx-TiO_2-130-NL, IrOx-TiO_2-150-NL and IrOx-TiO_2-170-NL; (c) IrOx-TiO_2-130-L, IrOx-TiO_2-150-L and IrOx-TiO_2-170-L; (d) oxygen generate rates of the studied samples and reference commercial P25-TiO_2 based samples; (e) the oxygen generation of IrOx-TiO_2-150-L based samples with theoretical 7%, 8%, 9% and 10% IrOx loading. Reaction conditions: 0.1g catalyst, 100 mL water solution, 1g AgNO3, LED-365 lamp.

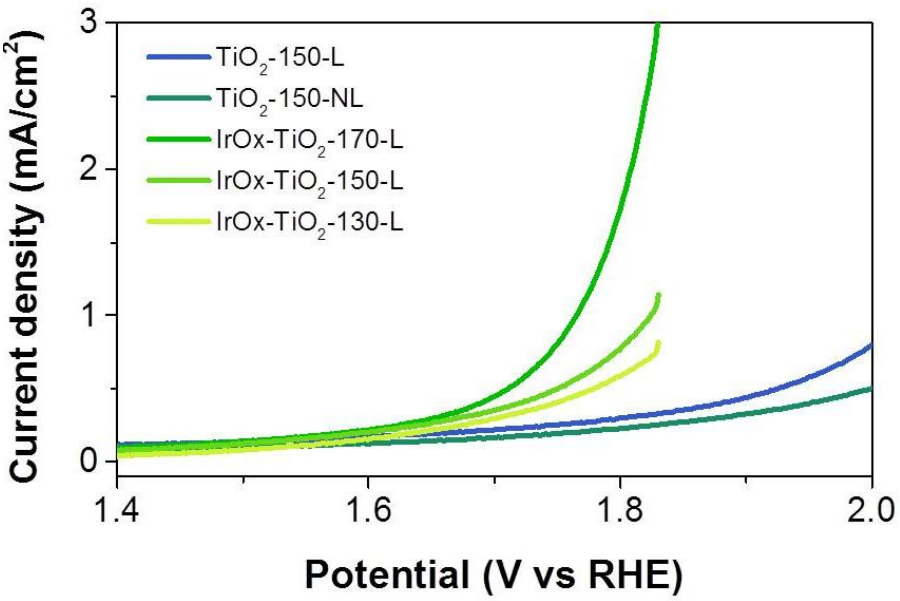

Figure S11. LSV plots of the samples under study. Conditions: 0.5 M Na_2SO_4, Ag/AgCl and Pt wire are employed as the reference and counter electrodes.

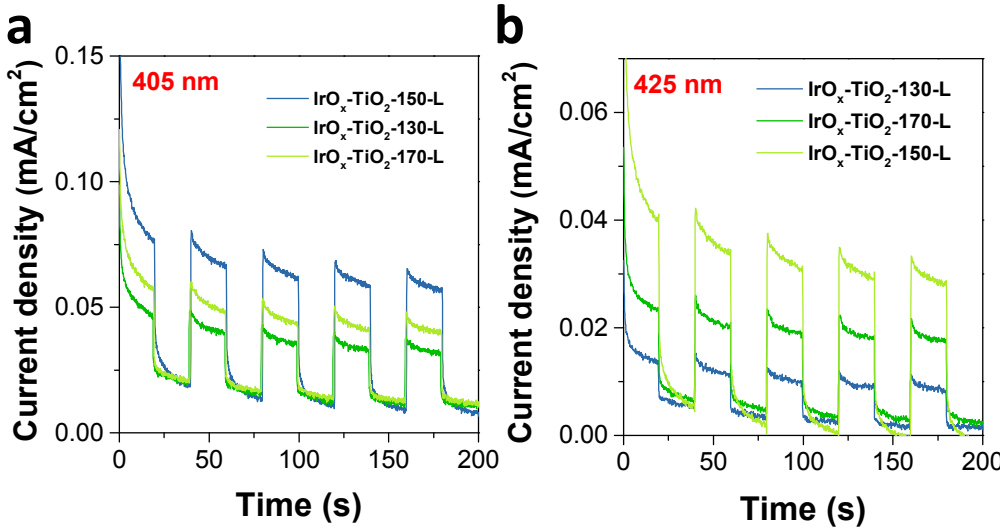

Figure S12. Photocurrent response under LED-405 and LED-425 nm lamps for the samples of IrOx-TiO_2-130-L, IrOx-TiO_2-150-L and IrOx-TiO_2-170-L, please note that a 1.2 V of bias voltage is used for the measurement.

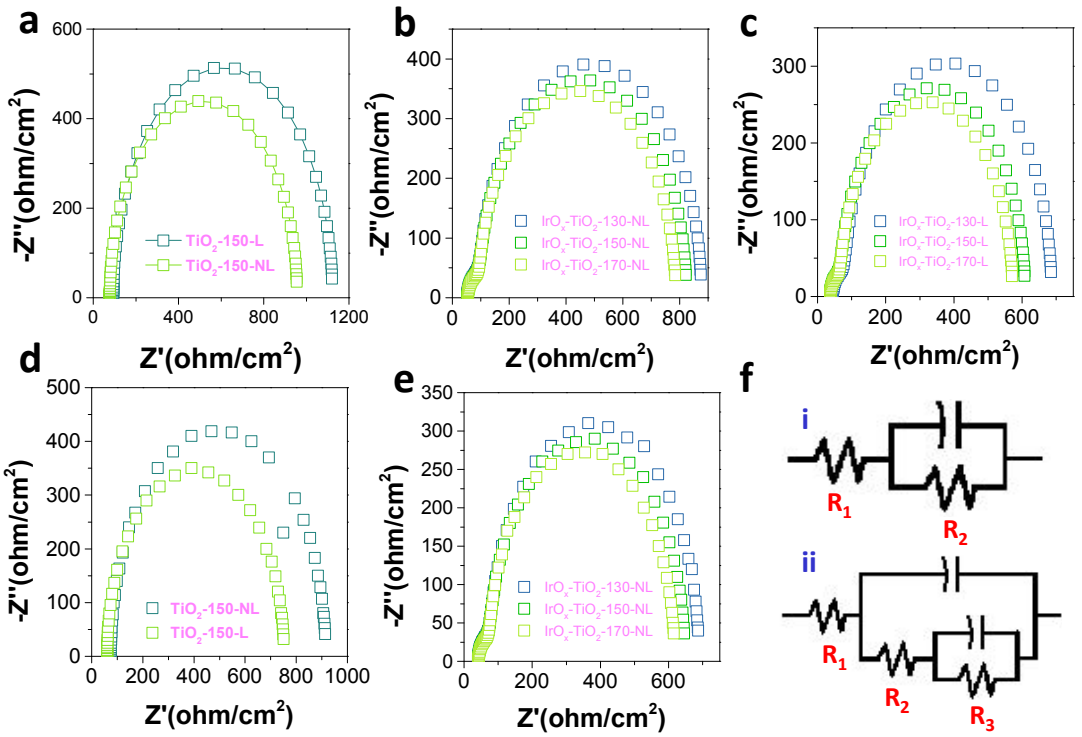

Figure S13. EIS plots. (a) and (d), the results of two samples of TiO_2-150-L and TiO_2-150-L under dark and LED-365 illumination conditions; (b) and (e), the results of three samples of IrOx-TiO_2-130-NL, IrOx-TiO_2-150-NL and IrOx-TiO_2-170-NL under dark and LED-365 illumination conditions; (c) the results of the three samples of IrOx-TiO_2-130-L, IrOx-TiO_2-150-L and IrOx-TiO_2-170-L under dark condition.

Table S2. The fitted values of the corresponding impedance (ohm/cm^2).

Sample	Without illumination			Under illumination		
	R_1	R_2	R_3	R_1	R_2	R_3
TiO_2-150-NL	94.9	1029	-	75.3	839.6	-
TiO_2-150-L	78.2	879.2	-	60.9	691.4	-
IrO_x-TiO_2-130-NL	54.1	73.72	744	41.6	61.9	585.6
IrO_x-TiO_2-150-NL	53.4	64.83	696	42.7	55.1	520
IrO_x-TiO_2-170-NL	54.8	69.9	661	42.2	58.1	547.4
IrO_x-TiO_2-130-L	45.1	61.5	580	29.7	43.6	413.7
IrO_x-TiO_2-150-L	37.1	51.2	483.3	27.4	38.2	358.8
IrO_x-TiO_2-170-L	37.6	54.6	517	30.1	40.95	386.7

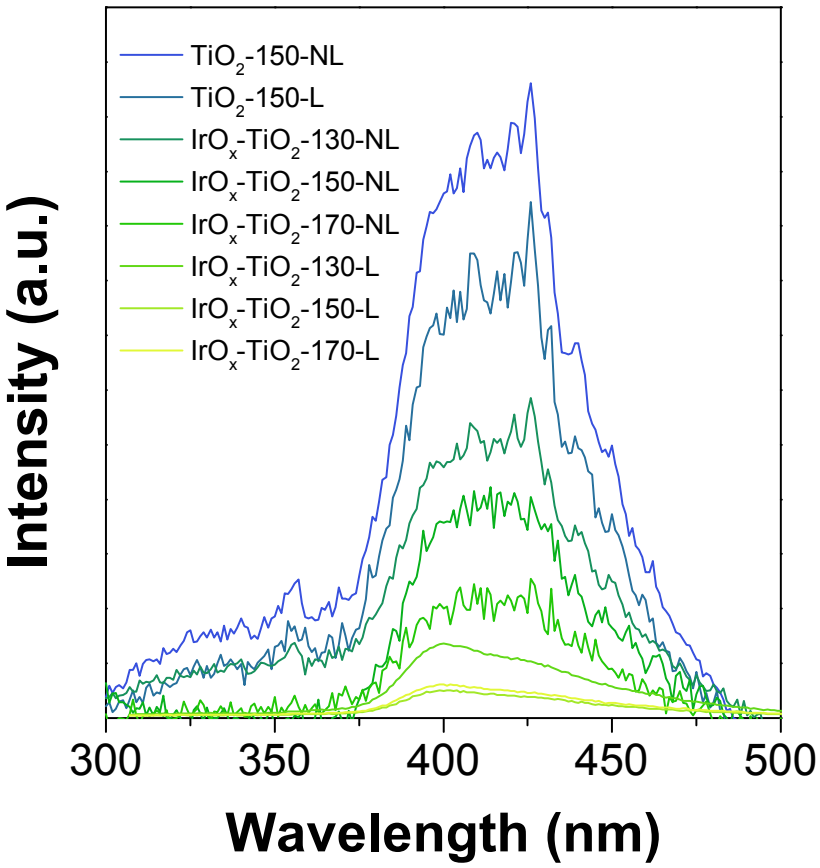

Figure S14. Room-temperature PL spectrum of the studied samples under the 295 nm incident light excitation.

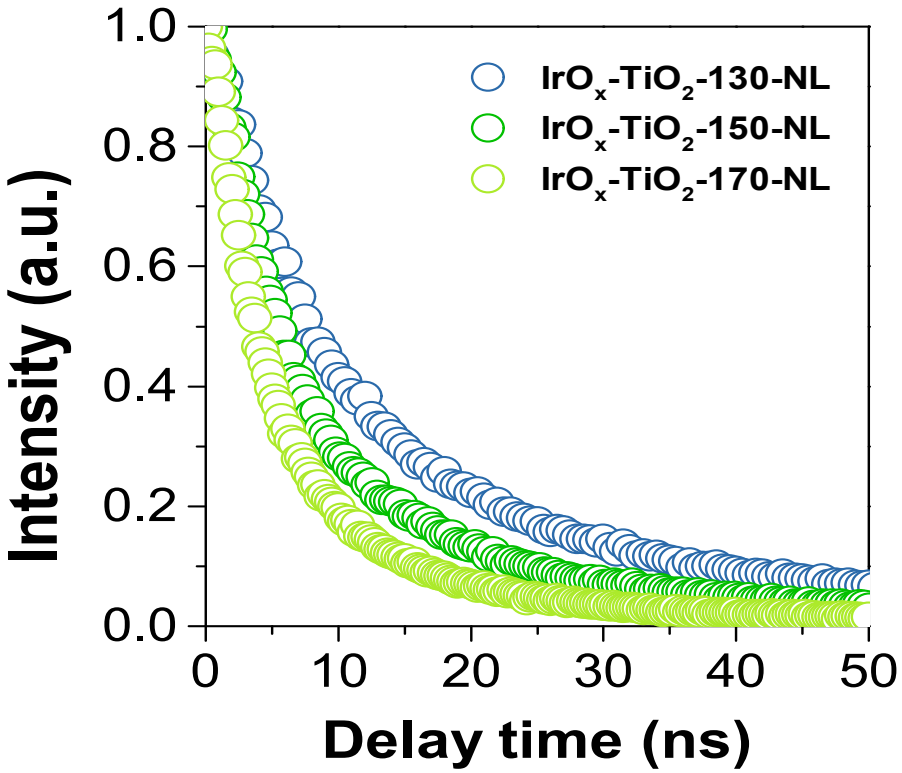

Figure S15. Time resolved fluorescence spectra of IrOx-TiO_2-NL samples (Excitation: 295nm, emission: 400 nm).

Table S3. The fitted values of the time parameters and the corresponding percents from the TRPL.

Sample	τ_1 (ns)	A_1 (%)	τ_2 (ns)	A_2 (%)	τ_{av}* (ns)
TiO_2-150-NL	46.7	16	9.7	84	27.39
TiO_2-150-L	32.8	17.5	5.6	82.5	20.67
IrO_x-TiO_2-130-NL	29.7	28.5	8.1	71.5	20.93
IrO_x-TiO_2-150-NL	27.4	22.5	5.8	77.5	18.29
IrO_x-TiO_2-170-NL	16.4	19.4	4.2	80.6	10.11
IrO_x-TiO_2-130-L	6.7	85.9	33.7	14.1	18.91
IrO_x-TiO_2-150-L	5.2	87.7	24.6	12.3	12.94
IrO_x-TiO_2-170-L	6.3	84.6	23.1	15.4	13.02

$*\tau_{av} = (\tau_1*\tau_1*A_1 + \tau_2*\tau_2*A_2) / (\tau_1*A_1+\tau_2*A_2)$